ISSN: 2583-9888
DOI: https://doi.org/10.51219/JAIMLD/Jia-Lin/13

URF PUBLISHERS
connect with research world

Journal of Artificial Intelligence, Machine Learning and Data Science

https://urfpublishers.com/journal/artificial-intelligence

Vol: 1 & Iss: 3

Research Article

Wheel-Rail Force Identification Method Based on CNN-BiLSTM Hybrid Model

He Jing[1], Zhong Qi[2], Jia Lin[2*], He Jia[3], Liu Hongyan[1]

[1]College of Electrical and Information Engineering, Hunan University of Technology, Zhuzhou 412007, China.

[2]College of Railway Transportation, Hunan University of Technology, Zhuzhou 412007, China.

[3]Guoneng Baoshen Railway Group Co., Ltd., Baotou 014010, China

Citation: Lin J, Qi Z, Lin J, Jia H, Hongyan L. Wheel-Rail Force Identification Method Based on CNN-BiLSTM Hybrid Model. *J Artif Intell Mach Learn & Data Sci*, 1(3), 100-108. DOI: https://doi.org/10.51219/JAIMLD/Jia-Lin/13

Received: 27 August, 2023; **Accepted:** 04 September, 2023; **Published:** 11 September, 2023

***Corresponding author:** Jia Lin, College of Electrical and Information Engineering, Hunan University of Technology, Zhuzhou 412007, China. Email: jialin@hut.edu.cn

ABSTRACT

Wheel-rail force is a key indicator for revealing the action between wheel and rail, describing the performance evolution laws of wheel sets and rails. The direct measurement method of wheel-rail force has a high cost, while the identification process of wheel-rail force based on mechanism models is cumbersome, computationally intensive, and of low accuracy. To solve these issues, a wheel rail force identification method based on the combination of vehicle dynamics response and convolutional long short-term memory network is proposed. Firstly, the feature set is constructed based on the vehicle vibration responses, vehicle body positions and attitudes, running status and other multi-source information, and further an effective feature subset is retained through feature selection to construct samples with multiple time step input and single time step output. Then, convolutional neural network (CNN) and bidirectional long short-term memory (BiLSTM) networks are combined to fully extract the spatio-temporal characteristics of wheel-rail force data. Finally, a fully connected layer is designed as the output wheel-rail force identification result. Taking the C80 vehicle as an example for analysis, the performance of the proposed method is evaluated from three aspects: model identification accuracy, generalization, and robustness. The results show that compared to traditional algorithms and single network models, the proposed method reduces the MSE value of wheel-rail lateral force identification by 44.4%~78.5%, and increases the R2 value by 1.3%~132.4%; the MSE value of wheel rail vertical force identification by 36%~75.9%, and the R2 value by 4.4%~87.9%. The proposed method can be applied to data of different working conditions and different noise levels.

Keywords: wheel-rail force identification; C80 vehicle; convolutional neural network; bidirectional long short-term memory network; different working conditions

CLC Number: TN0;TP183 **Document Identification Code:** A **National Standard Subject Classification Code:** 510.40

Introduction

The development of railway transportation continues to head towards the direction of high speed, heavy load, multi-system, and new structure[1], resulting in various operating conditions and complex wheel-rail interactions. To secure safe operations of train, it is of great importance to reveal the relationships between wheels and rails, more specifically, to obtain high-precision data of wheel-rail force. Therefore, this issue has been extensively and deeply studied in recent years[2-3]. At present, the measurement methods of wheel-rail force mainly include direct measurement method and indirect measurement method. The direct measurement uses the force-measuring wheel set to obtain wheel-rail force. The measurement accuracy is high. However, due to the structural characteristics and cost of the force-measuring wheelset, it is difficult to install it on all vehicles. Moreover, the installation, calibration, and data acquisition of the force-measuring wheelset is quite complicated. The cost of operation and maintenance is high, and the measurement period is long. Thus, the actual application of force-measuring wheelset is limited[4-6]. The indirect measurement method takes the wheel-rail force as the input of the vehicle dynamic system, and takes the vibration response of each component of the vehicle as

Received Date: August 2023

***Funded Projects:** Funded by the National Key Research and Development Program (2021YFF0501101), the National Natural Science Foundation of China (62173137, 52172403,62303178)

the output. The algorithm model is used to learn the mapping relationship between wheel-rail force and the vibration response, so that wheel-rail force can is identified[7-11] through the measured vibration response. The indirect measurement methods are mainly divided into models based on the mechanism and models based on data.

For researches on indirect measurement wheel-rail force based on mechanism model, Uhl[12] used Bellman dynamic programming theory to identify the wheel-rail force. Ronasi H et al.[13] proposed a strain measurement based wheel-rail contact force estimation method. It determined the wheel-wheel contact force by minimizing the least square difference between the measured radial strain and the corresponding calculated strain in the three-dimensional finite element model of the wheel. Pedro Urda et al.[14] applied strain gauges and distance lasers to measure wheel-rail force on railway vehicles. Based on the theory of structural dynamics, Zhu Tao et al. utilized Duhamel integral and combined with the characteristics of the rail vehicle system to derive the analytical load identification methods. Wu J et al.[15] discussed a Truncated Singular Value Decomposition (TSVD) parameter selection method based on Wilson- method and minimum response error principle. It improved the accuracy of wheel-rail force identification. Wang Mingmeng et al.[16] used the inverse structural filtering method to identify wheel-rail force with structural response parameters as input. Zhou Yabo[17] adopted the Kalman filtering technology to the wheelset lateral-vertical coupling model, and used the vibration acceleration of the railway vehicle to identify wheel-rail force. The deduction process of the method based on the mechanism model is rather complex, with a large amount of calculation. Due to the limitation of the equations, a model has to be built for each different working condition to obtain output results of the wheel-rail force. The adaptability to complex and various working conditions is therefore restricted.

The development of artificial intelligence algorithms and vehicle system sensor technology provides a wealth of algorithms and data support for the data-based wheel-rail force identification method[18-19]. A technology proposed by Li Y et al.[20] can continuously monitor the wheel-rail contact force. It adopted the radial basis function network model and provided a new approach for the researches on wheel-rail force identification. Zhang Ranjia et al.[21] made use of the BP neural network to learn the mapping relationship between the force-measuring wheelset bridge output and wheel-rail force, and optimized the network with a genetic algorithm to perform the identification of wheel-rail force. Urda P et al.[22] demonstrated an experimental measurement method of wheel-rail lateral contact force based on artificial neural network (ANN), and used artificial neural network to identify the lateral contact force between the wheel and the track. Teng F et al.[23] illustrated a lightweight wheel-rail force inversion model (LFIM). It was based on convolutional neural network and adopted vibration signals collected from vehicle systems to identify wheel-rail force at flat line and curved track running conditions. Pires AC et al.[24] used a machine learning model to indirectly identify the wheel-rail contact force of heavy-haul railway vehicles. A tree-based pipeline optimization tool (TPOT) trained and optimized a total of 24 embedded machine learning models, and selected the optimal model to perform wheel-rail force identification. To sum up, most of the current researches are carried out with simple neural network models, a better accuracy is still in great need. In addition, the above studies are often limited to the study of preset data sets, and lack of consideration of different working conditions and different signal-to-noise ratio data. Therefore, the generalization and robustness of the model need to be improved.

Hence, a data-driven wheel-rail force identification model is proposed in this paper, and its identification performances for the wheel-rail force at different working conditions and different signal-to-noise ratios are analyzed. This model adopts deep learning algorithm, and uses the collected vibration response data to establish the mapping relationship between variables and the wheel-rail force. In this way, the wheel-rail force is identified. The main contributions of this paper are as follows:

1. A multiple time step input and single time step output database is established, covering information such as vehicle vibration response, vehicle body position and attitude, running status, as well as wheel-rail force data. A Filter-Wrapper feature screening algorithm is proposed. Combining the rapidity of Filter feature screening algorithm with the high accuracy of Wrapper feature screening algorithm, the feature dimension is effectively reduced and redundant features are deleted.
2. A wheel-rail force identification method is designed to combine one-dimensional convolutional neural network and bidirectional long short-term memory network. It integrates the advantage of CNN in digging data out of discontinuous data in high dimensional space with the advantage of BiLSTM in capturing hidden information of time series data, and therefore obtains enhanced ability of extracting data features.
3. A variety of model performance evaluation indicators are proposed, covering the model identification accuracy, the application performance of the evaluation model at different operation conditions and the anti-interference performance with input data of different signal-to-noise ratios.

1. Wheel-rail force identification model

In this paper, the wheel-rail lateral force and vertical force are taken as the research objects, and the wheel-rail forces are identified based on the vibration responses generated by the railway vehicle system during operation. The framework of the model system is shown in **Fig. 1**. Firstly, a rigid-flexible coupled multi-body dynamic model of vehicle-rail is established by using dynamics software. Then, the dynamic model is used to simulate the real vehicle data at different working conditions of typical scenes such as operations on small curvature track and flat railway line. After data preprocessing and feature selection, the effective features are extracted as the input sample, and the wheel-rail force is taken as the label of the sample to construct a sample set of multiple time step input and single time step output. Finally, the end-to-end wheel-rail force identification model between the vibration response, vehicle body position and attitude, running status data of railway vehicles and the wheel-rail force is established by using such sample data sets.

1.1 Establishment of dynamic model and selection of features

The method proposed in this paper is verified with data of a C80 heavy-haul train. For the C80 train, various physical parameters of the bogie were tested on the rolling test bench, and the structural characteristic parameters of the vehicle were measured based on the standard experiment. A dynamic model was established for it by using a dynamics software. The feasibility and accuracy of this model were verified by comparing its results with the vehicle's response at actual line conditions. This model is used to construct the initial data set of vehicle response under different working conditions. The data

set mainly includes the vehicle vibration response, vehicle body position and attitude, running status, wheel-rail force and other information. **Fig. 2** shows positions of virtual sensors on some vehicle components in this dynamic model.

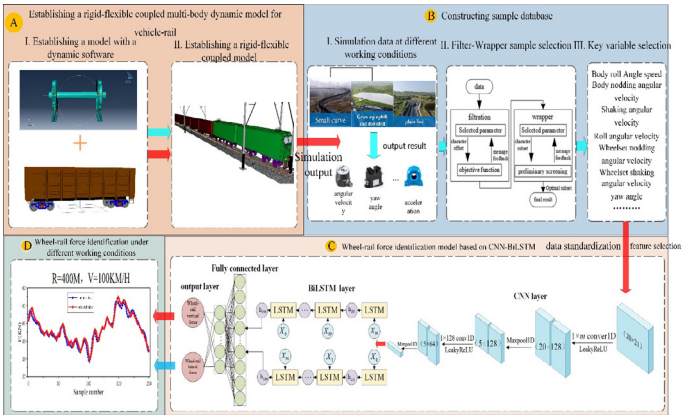

Figure 1: Framework diagram of model system.

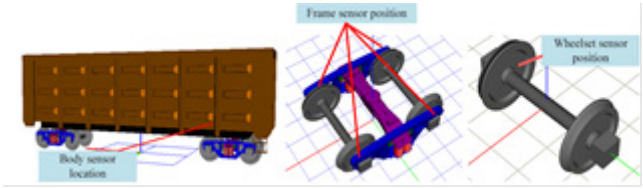

Figure 2: Positions of virtual sensors in the dynamic model.

In order to effectively improve the performance of network training, the multi-source data were normalized or standardized to convert them into dimensionless index evaluation values. Due to the complex and diversified working conditions during the train operation, there would be abnormal fluctuation values and extreme deviation values in the data, which would reduce the effect of data normalization. Therefore, this paper used the Z-Score standardization method[25] to process the data and the calculation formula is as follows:

$$x' = \frac{x - \mu}{\sigma} \qquad (1)$$

In formula (1), is the converted z-score, is the original score value, μ is the mean score value of the overall sample space, then is the standard deviation of the overall sample space.

In vehicle systems, sensors are used in a wide range of applications, from radar, accelerometers, displacement sensors to gyroscopes. With data collected from each sensor, a complete, representative sample can be built. However, because of the wide variety of sensors and the different mounting locations of each sensor, it is extremely difficult to obtain accurate original features.

By introducing two combined algorithms of Filter and Wrapper[26], irrelevant features in the input data can be effectively reduced, thereby greatly improving the operating efficiency of the model and helping to reduce the occurrence of dimensionality hazard. Filter is an effective method. It can effectively reduce incoherent features, thereby reducing the dimensionality of features. The Wrapper method is used to screen out the valid information, so as to eliminate redundant information. Filter method is based on mutual information. It can detect the interaction between various information and markers, whether positive or negative, and its formula is as follows:

$$I(X;Y) = \sum_{x \in X} \sum_{y \in Y} p(x,y) \log \frac{p(x,y)}{p(x)p(y)} \qquad (2)$$

In equation (2), $p(x)$ represents the probability that $X=x_i$ occurs, and $p(y)$ represents the probability that $Y=y_i$ occurs. $p(x,y)$ represents the probability that $X=x_i$ and $Y=y_i$ occur simultaneously, that is, the joint probability. $I(X;Y)$ denotes mutual information measures the information shared by two random variables.

The return value is between 0 and 1, with 0 indicating that the two features are not connected at all and 1 indicating that the two features are very close. The accuracy of the feature subset was ensured by four steps: (1) extracting out the best feature subset; (2) evaluating the goodness of the best feature subset; (3) confirming the optimal solution; (4) checking the reliability of the feature subset.

Taking the carbody and front bogie as the research objects, the parameter characteristics of the vehicle system were preliminarily screened based on the feasibility and convenience principle of collecting various parameter characteristics in practical engineering applications, and then the Filter-Wrapper algorithm was used to remove invalid redundant characteristics; Finally, 21 parameter features that are easier to measure and have a greater influence on wheel-rail force were retained as the input for wheel-rail force identification, as shown in X1~ X21 in Table 1. The wheel-rail lateral force and vertical force were considered to be output of the model, that is, FL and FQ in **Table. 1**.

Table 1: Features and Label Settings.

Signal type	State parameter	Symbol
Vibration response	Lateral acceleration of the left frame	X_1
	Lateral acceleration of the right frame	X_2
	Vertical acceleration of the left frame	X_3
	Vertical acceleration of the right frame	X_4
	Lateral acceleration of bolster	X_5
	Vertical acceleration of bolster	X_6
	Wheelset lateral acceleration	X_7
	Wheelset vertical acceleration	X_8
	The displacement of the wheel with respect to the track	X_9
	Lateral angular displacement of wheelset	X_{10}
	Vertical angular displacement of wheel set	X_{11}
Body position	Body roll Angle speed	X_{12}
	Body nodding angular velocity	X_{13}
	Body shaking angular velocity	X_{14}
	Angular speed of wheel to side roll	X_{15}
	Wheelset nodding angular velocity	X_{16}
	Wheelset shaking angular velocity	X_{17}
Running status	yaw angle	X_{18}
	Lateral winding of wheel and rail	X_{19}
	Vertical winding of wheel and rail	X_{20}
	Wheel-rail torsional winding	X_{21}
Wheel-rail (force (output	Wheel-rail lateral force	F_L
	Wheel-rail vertical force	F_Q

Construction of sample set and network design

After construction the feature set with selected features, a sample data set of multiple time step input and single time step output is established. After normalization, m channel data were spliced, intercepted and slid to construct samples for l×m time series input and 2 output. The label of each sample was wheel-rail force response, and its features include vehicle body position and attitude, running status information, and the vibration response at l time steps before and after this moment. Compared

with the samples corresponding to only single-time input and output, the sample construction method in this paper fully considers the uniqueness of the timing signal, and fully retains the complete time-dimensional characteristic information in each sample through the time clip sampling method. Compared with the characteristic prediction output of a single time step, this construction method can effectively prevent issues such as the phase difference between multiple measuring points, the time lag between the input and output of the dynamic system, and the abnormal damage of the data of a single time step. The sample was constructed as shown in **Fig. 3**.

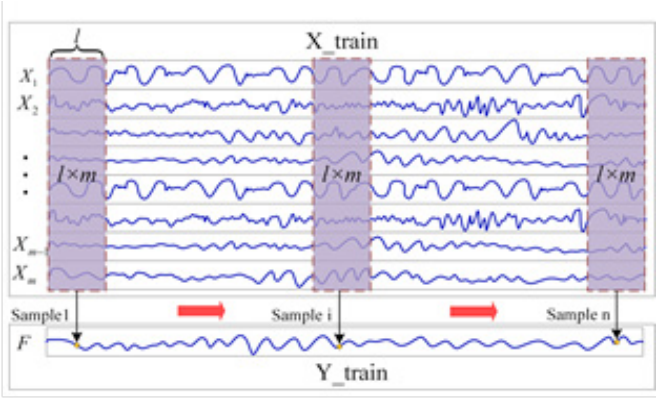

Figure 3: Construction of sample set

For the lack of ability of the single network model CNN[27] to extract hidden information of time series data and the disadvantage of the BiLSTM network[28] in capturing discontinuous data features in high-dimensional space, CNN and BiLSTM were fused to form a CNN-BiLSTM hybrid model. It not only has the ability of CNN model to extract spatial features, but also can call the ability of BiLSTM model to extract temporal features[29]. As the change of parameters in the training process will lead to a large change in the data distribution of each layer, this paper added a BN layer to constrain the data distribution to improve the convergence and training rate of the network. At the same time, the Dropout layer was introduced to randomly block the output of some neurons. In order to adapt to the sparse gradient and alleviate the gradient oscillation, so that the model can better learn the mapping relationship between input and output, the Adam optimization algorithm is adopted. The designed network structure of CNN-BiLSTM hybrid model is shown in **Fig. 4**.

The input of a single sample contains time series data of 21 channels and 1000 time steps, generating wheel-rail force values of intermediate time points. In order to make full use of the data, sliding sampling was carried out on the input sample, with a sampling window size of 20×21 and a step size of 1. A total of 980 groups of 20×21 small fragments arranged in chronological order were obtained. For these small fragments, two rounds of convolution and maximum pooling operations were carried out respectively to extract the spatial characteristics of the data. Two convolution operations were performed using a one-dimensional convolution kernel with a size of [1, 1] and a step size of 1. The depth of the first convolution was 21 and the depth of the second convolution was 128. LeakyReLU activation function was adopted. The size of the largest applied pooling layer was [2,1] and step size was 1. No padding was applied during convolution and pooling, resulting characteristic data of 64 channels. These 980 sets of characteristic data input of 64 channels were transmitted into the BiLSTM layer to bidirectionally extract the potential information of timing data. The number of hidden units of the BiLSTM layer was initially set to 20. Finally, data were input into three fully connected layers, and a Dropout rate of 0.2 was applied. The number of cells in the fully connected layer was set to 64, 8, and 1, respectively, to produce an identified value output of wheel-rail force.

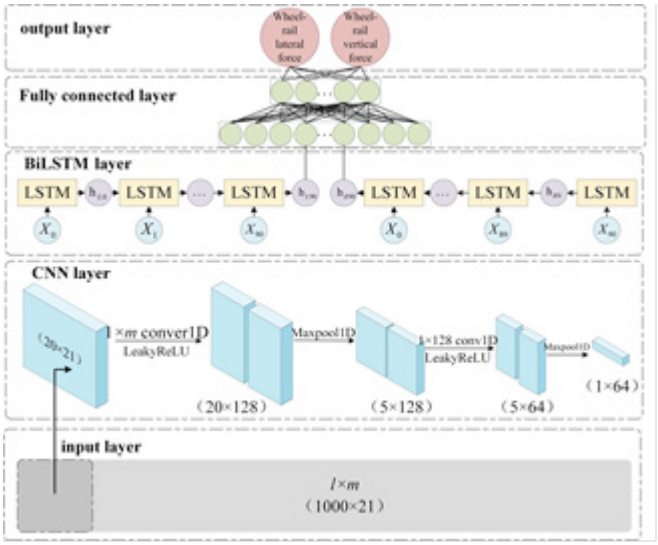

Figure 4: Structure of wheel-rail force identification network integrating CNN and BiLSTM.

Experiment Result Analysis

The experimental results are presented and analyzed here. The experiment consists of 3 parts. Part 1 was a comparative analysis of the accuracy and error of different wheel-rail force identification models. The wheel-rail force identification performance of the proposed CNN-BiLSTM model was compared with that of other wheel-rail force identification models. Part 2 verified the generalization performance of CNN-BiLSTM model and analyzed the wheel-rail lateral force identification performance of the model at different working conditions; Part 3 validated the practicability of CNN-BiLSTM model, and compared and analyzed the identification results with data of different noise degrees.

The experiment was carried out with a 64-bit Windows 10 system, a Python 3.7 integrated development environment, CPU AMD Ryzen 7 5800H with Radeon Graphics 3.20 GHz, and a16GB DDR4 3200MHZ running memory. The model parameters were set as described in Section 2.2. In this section, the signal-to-noise ratio of the original data was 6db, the running condition was a speed of 60 km/h and a curvature of 400 m radius, the data sampling frequency was 200 Hz, and the track irregularity excitation input of this dynamic model simulation was the US Class 5 track frequency.

In the experiment, the mean square error (MSE)[29] was selected as the loss function in the network training process, and its calculation was performed as follows:

$$MSE(\hat{y}, y) = \frac{1}{n}\sum_{i=1}^{n}(y^{(i)} - \hat{y}^{(i)})^2 \quad (3)$$

At the same time, the coefficient of determination R2 score[29] was used to evaluate the accuracy of the model, and it was determined by below equation:

$$R^2 = 1 - \frac{\frac{1}{n}\left(\sum_{i=1}^{n}(y^{(i)} - \hat{y}^{(i)})^2\right)}{\frac{1}{n}\left(\sum_{i=1}^{n}(y^{(i)} - \bar{y}^{(i)})^2\right)} = 1 - \frac{MSE(\hat{y},y)}{Var(y)} \quad (4)$$

In equation (3) and (4), $y^{(i)}$ * MERGEFORMAT is the predicted data, $\hat{y}^{(i)}$ * MERGEFORMAT is the original data, and n is the number of samples.

Comparative experiment

In order to verify the effectiveness of the CNN-BiLSTM model proposed in this paper, it was compared with 7 other wheel-rail force identification models of CNN[27], BiLSTM[28], GRU[30], SVM[31], GDBT[32], XGBOOST[33], and decision tree regression.

Comparative experiment on identification performances for wheel-rail lateral force

The wheel-rail lateral force were identified with above-mentioned 8 different models. The changes of error and accuracy with time on training data of CNN, BiLSTM, GDBT, CNN-BiLSTM are shown in **Fig. 5 (a)**, and the changes of error and accuracy on test data with time are shown in **Fig. 5 (b)**. Hereby, a training cycle refers to the process of inputting all data into the network to complete a forward propagation and error backpropagation.

In **Table. 2**, the MSE and R2 index results of each model on the training set and test set in the last training cycle are listed. It can be seen clearly from **Table. 2** that the difference between the error on the test set and the one on the training set is small, for each wheel-rail force identification model. The identification performances of both CNN and BiLSTM single models on wheel-rail lateral force are worse than that of CNN-BiLSTM. This indicates that the hybrid model has better identification ability than the single model. The errors of BiLSTM model are greater than those of CNN model. This is due to the influence of a large amount of noise on the original sample data. By using the convolutional neural network and multi-time step input sample construction, the characteristics of the time period can be effectively extracted, thus resisting the interference to a certain extent. With the same noise level of data environment, the CNN-BiLSTM model proposed in this study reaches an MSE of 0.1113 on the final test set. This value is reduced by 44.4%~78.5% compared with those of other models; Meanwhile, its R2 value is 0.8133, increased by 1.3%~132.4% compared with those of other models. The above results demonstrate that the identification error of the proposed model is smaller than those of other models when dealing with the data of actual working conditions containing noise signals.

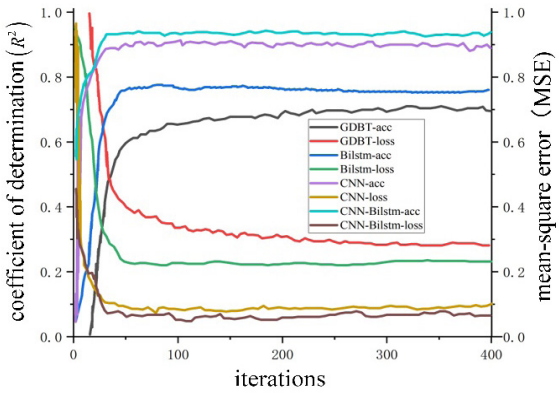

(a) Training set

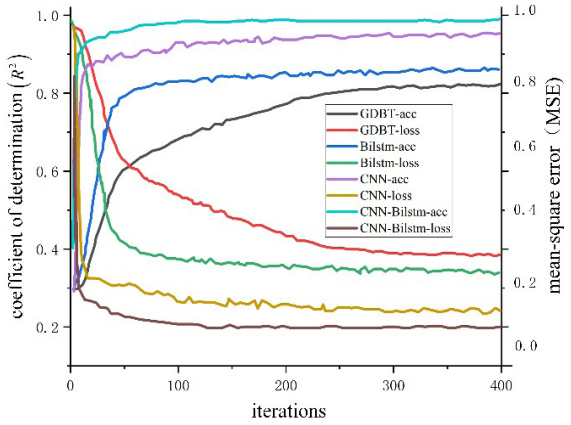

(b) Test set

Figure 5: Errors and accuracies of different models (wheel rail lateral force).

Table 2: Comparison of errors and accuracies of different models (wheel rail lateral force).

Model	Training set		Test set	
	MSE	R^2	MSE	R^2
CNN	0.0879	0.9143	0.2137	0.6342
BiLSTM	0.2715	0.8009	0.3690	0.3499
GRU	0.2613	0.8235	0.3568	0.4398
SVM	0.3165	0.7998	0.5169	0.4136
GDBT	0.2911	0.8190	0.3005	0.6871
XGBOOST	0.1569	0.9136	0.2003	0.8031
Decision tree regression	0.2913	0.8333	0.3106	0.6789
Mentioned herein CNN-BiLSTM	0.0576	0.9613	0.1113	0.8133

Comparative experiment on identification performance of wheel-rail vertical force

In order to verify the applicability of the model in identifying wheel-rail force at different working conditions such as flat line, small curvature line, long uphill and downhill slopes, 18 working conditions and 16 different long uphill and downhill slopes with straight lines and curvature radii of 400 m, 600 m, 800 m, 1000 m and 1200 m at the running speeds of 60 km/h, 80 km/h and 100 km/h were simulated, respectively. Taking wheel-rail vertical force identification as an example, the identification performance of this model at the above 34 working conditions was explored under the same noise environment and track irregularity excitation. Among them, 12 kinds of identification performances are shown in Fig. 7. It can be seen that the proposed model can better fit the change trend of vehicle wheel-rail force at different working conditions. Table 4 shows the root mean square error MSE and coefficient of determination R2 indicators obtained by the CNN-BiLSTM model at different working conditions with flat line and small curvature track. It can be seen that R2 of the proposed model is above 0.91 and the MSE is below 0.1 with curved track conditions at different operating speeds and different curvature radii. Combining the data given in **Table. 5**, it can be seen that although the wheel-rail force identification accuracies for working conditions of flat line and small curvature track are slightly worse, the overall performance of the model is better, as R2 is above 0.89 and MSE is below 0.2. To sum up, it can be concluded that the proposed model has high wheel-rail force identification accuracy, strong generalization ability, and is suitable for different working conditions.

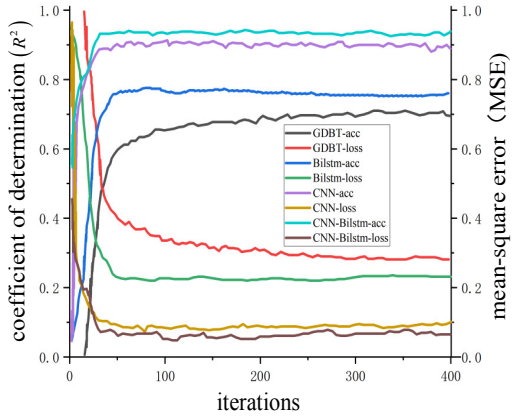

(a) Training set

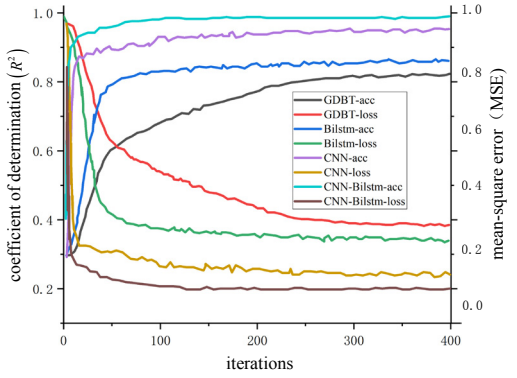

(b) Test set

Figure 6: Errors and accuracies of different models (wheel rail vertical force)

Table 3: Comparison of errors and accuracies of different models (wheel rail vertical force).

Model	training set		Test set	
	MSE	R^2	MSE	R^2
CNN	0.0781	0.9005	0.2081	0.6236
BiLSTM	0.2813	0.8111	0.372	0.4913
GRU	0.1613	0.8465	0.3721	0.4612
SVM	0.3301	0.7818	0.5061	0.4266
GDBT	0.2311	0.8391	0.3125	0.6915
XGBOOST	0.1439	0.9188	0.1903	0.7681
Decision tree regression	0.2812	0.8133	0.3098	0.6833
Mentioned herein CNN-BiLSTM	**0.0636**	**0.9699**	**0.1218**	**0.8016**

Evaluation of model generalization performance

In order to verify the applicability of the model in identifying wheel-rail force at different working conditions such as flat line, small curvature line, long uphill and downhill slopes, 18 working conditions and 16 different long uphill and downhill slopes with straight lines and curvature radii of 400 m, 600 m, 800 m, 1000 m and 1200 m at the running speeds of 60 km/h, 80 km/h and 100 km/h were simulated, respectively. Taking wheel-rail vertical force identification as an example, the identification performance of this model at the above 34 working conditions was explored under the same noise environment and track irregularity excitation.

Table 4: Prediction error and accuracy under different working conditions.

车?	线路	外轨实设超高	MSE	R^2
V=60km/h	直线		0.0587	0.9304
	R=400m	188mm	0.0656	0.9301
	R=600	125	0.0683	0.9208
	R=800	94	0.0576	0.9281
	R=1000	75	0.0638	0.9500
	R=1200	63	0.0863	0.9108
V=80km/h	直线		0.0473	0.9351
	R=400m	188mm	0.0816	0.9199
	R=600	125	0.0395	0.9549
	R=800	94	0.0491	0.9417
	R=1000	75	0.0317	0.9605
	R=1200	63	0.0431	0.9689
V=100km/h	直线		0.0531	0.9403
	R=400m	188mm	0.0483	0.9516
	R=600	125	0.0531	0.9613
	R=800	94	0.0419	0.9514
	R=1000	75	0.0387	0.9619
	R=1200	63	0.0399	0.9589

Among them, 12 kinds of identification performances are shown in **Fig. 7**. It can be seen that the proposed model can better fit the change trend of vehicle wheel-rail force at different working conditions. **Table. 4** shows the root mean square error MSE and coefficient of determination R2 indicators obtained by the CNN-BiLSTM model at different working conditions with flat line and small curvature track. It can be seen that R2 of the proposed model is above 0.91 and the MSE is below 0.1 with curved track conditions at different operating speeds and different curvature radii. Combining the data given in **Table. 5**, it can be seen that although the wheel-rail force identification accuracies for working conditions of flat line and small curvature track are slightly worse, the overall performance of the model is better, as R2 is above 0.89 and MSE is below 0.2. To sum up, it can be concluded that the proposed model has high wheel-rail force identification accuracy, strong generalization ability, and is suitable for different working conditions.

Assessment of model robustness

During the actual operation of the train, the signals collected by sensors are affected by noise. Especially in the case of poor track conditions, the noise content will increase significantly, and affect the identification performance of wheel-rail force models. Therefore, in order to have greater engineering application value and practical significance, and maintain good performance, the wheel-rail force identification model should be able to effectively overcome noise interference with different intensities, should be of excellent robustness, adapt to various noise environments and maintain a stable working state.

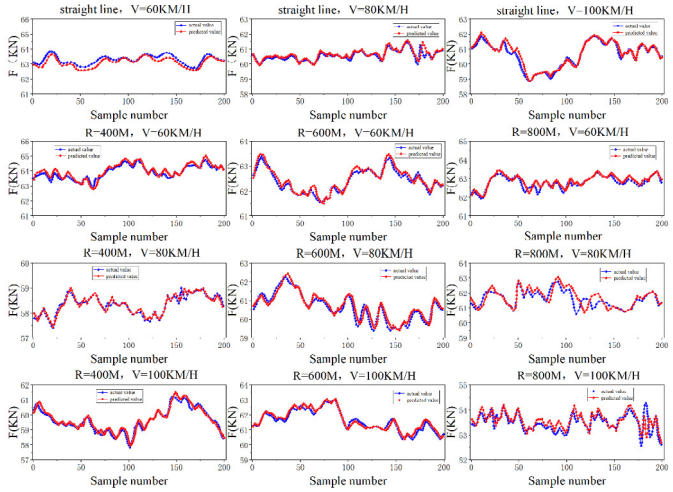

Figure 7: Prediction performance for wheel-rail vertical force at different working conditions.

Table 5: Prediction error and accuracy of different working conditions with long uphill and downhill slop

speed (km/h)	Length of relaxation curve (m)	radius of vertical curve (m)	slope (°)	Clip length (m)	MSE	R^2
60	120	1500	20	12.5	0.1436	0.9126
				25	0.1355	0.9308
				37.5	0.1175	0.9265
				50	0.1241	0.8975
				62.5	0.1163	0.8889
				80	0.1079	0.9075
				92.5	0.1369	0.9268
				110	0.1277	0.9109
80	120	1500	10	12.5	0.1581	0.8997
				25	0.1132	0.9103
				37.5	0.1218	0.8706
				50	0.0991	0.9013
				62.5	0.1018	0.9226
				80	0.1109	0.9088
				92.5	0.0989	0.9153
				110	0.1087	0.9009

When the signal-to-noise ratio decreased from 1000 dB to 1 dB, the MSE and R2 values of the four kinds of models had significant changes. MSE became lower than 0.1, while the R2 value was higher than 0.9, indicating a strong identification. In addition, when the signal-to-noise ratio was 100 dB, the identification ability of these models was also significantly improved. When the signal-to-noise ratio was less than 100 dB, the accuracy of GDBT and LSTM models would drop sharply, and might even reach extremely low levels; In contrast, the accuracy of CNN and the CNN-BiLSTM model proposed in this paper would also be affected, but by a relatively small extent and could still maintain a high prediction accuracy level. When the signal-to-noise ratio reached 1 dB, R2 values of GDBT, BiLSTM, CNN and CNN-BiLSTM models were 0.1623, 0.1733, 0.6571 and 0.7495, respectively. The identification ability of CNN-BiLSTM model is the best, which shows that the proposed model is of good robustness in harsh noise environments, and capable of effectively identifying the wheel-rail force.

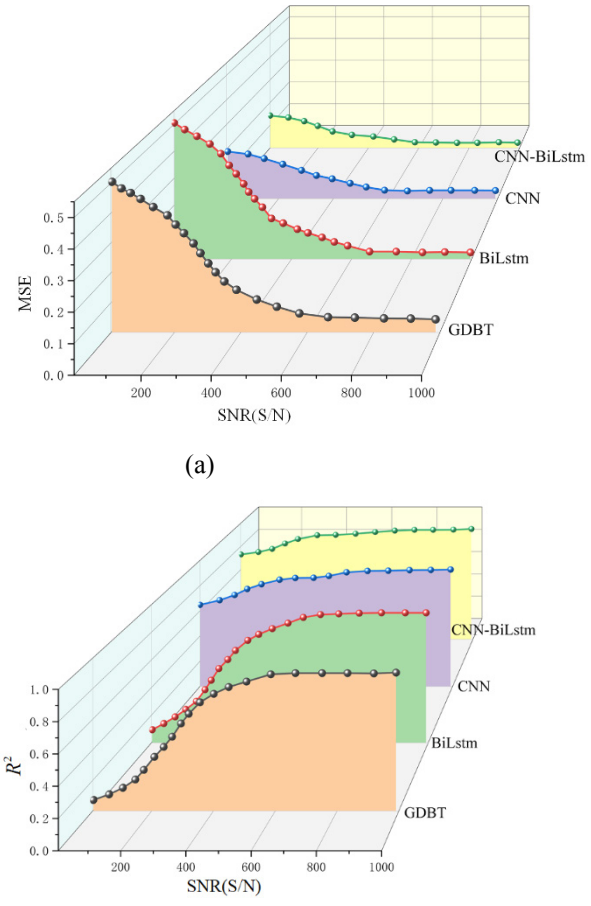

Figure 8: Error and accuracy of each model under different signal-to-noise ratios

Conclusions

Against the issues of high cost and complex process for wheel-rail force direct measurement, of tedious deduction process and large calculation amount for mechanism model-based models, a data-driven wheel-rail force identification method is proposed based on multi-source information such as vehicle vibration response, vehicle body position and attitude, and running status. Based on the simulation data of a dynamic model, a multi-source information database of vehicle dynamic response is established, and the Filter-Wrapper filtering feature algorithm is used to better retain the valid features of the data. Data of a C80 freight train is taken as an example, based on the above database. A data-driven wheel-rail force identification model CNN-BiLSTM containing physical information is established to identify the wheel-rail force of heavy-haul train at 34 different working conditions of straight line, small curvature, long uphill and downhill slope, etc. The experiment results show that the proposed method can identify the wheel-rail force with higher accuracy. The performance of it is better than that of traditional identification algorithms and the single network models. It has the ability to identify wheel-rail force at various working conditions and in harsh noise environments, therefore it is of practical value for actual engineering applications. Although the end-to-end wheel-rail force identification model has lower wheel-rail force measurement cost and simpler deduction process, the data-driven identification algorithm is a black box model, so the interpretability of the method proposed in this paper needs to be further studied.

References

1. Zhu T, Xiao S N, Yang G W. State-of-the-art development of load identification and its application in study on wheel-rail forces[J]. Journal of the China Railway Society 2011;33(10):29-36.
2. Wu P, Zhang F, Wang J, Wei L, Huo W. Review of wheel-rail forces measuring technology for railway vehicles[J]. Advances in Mechanical Engineering 2023;15(3):16878132231158991.
3. Luo R, Shi H, Teng W, Song C. Prediction of wheel profile wear and vehicle dynamics evolution considering stochastic parameters for high-speed train[J]. Wear 2017;392:126-138.
4. Ran D, Qiang L, Zunsong R. Statistics characters of wheel/rail loads of intercity EMU[J]. Journal of Mechanical Engineering, 2019;55(6):108-115.
5. Wu P, Zhang F, Wang J, et al. Review of wheel-rail forces measuring technology for railway vehicles[J]. Advances in Mechanical Engineering, 2023;15(3):16878132231158991.
6. He Qing; Li Chenzhong; Ma Yusong; Wang Ping; Yu Weidong; A gift from heaven; Wang Qihang; Wang Xiaoming; High rock; Wang Jianhui; Lilu; Sun Huakun; A dynamic orbit fine-tuning method based on particle swarm optimization, 2021-1-29, China, ZL202011238831.4
7. Xia F, Colin C, and Peter W. An inverse railway wagon model and its applications. Vehicle system dynamics 2007;45(6):583-605.
8. Xia F, Colin C, and Peter W. Grey box-based inverse wagon model to predict wheel–rail contact forces from measured wagon body responses. Vehicle System Dynamics 2008;46. S1:469-479.
9. Tao Z, Shoune X, Guangwu Y. A new time-domain method for force identification[J]. Journal of Southwest Jiaotong University 2012;47(6):968-973.
10. Kaijuka PL, Dixon R, Ward CP, Dutta S, Bemment S. Model-based controller design for a lift-and-drop railway track switch actuator[J]. IEEE/ASME Transactions on Mechatronics 2019;24(5):2008-2018.
11. Shan-chao S, Jin-zhao L, Wei-dong W, Xiao-ming L, Yue-guang W. Holographic identification model of wheel & rail contact force for hihg-speed railway[J]. engineering mechanics 2018;35(11):190-196.
12. Uhl T. The inverse identification problem and its technical application[J]. Archive of Applied Mechanics 2007;77:325-337.
13. Ronasi H, Johansson H, Larsson F. Identification of wheel–rail contact forces based on strain measurements, an inverse scheme and a finite-element model of the wheel[J]. Proceedings of the Institution of Mechanical Engineers, Part F: Journal of Rail and Rapid Transit 2014;228(4):343-354.
14. Urda P, Muñoz S, Aceituno JF, Escalona JL. Wheel-rail contact force measurement using strain gauges and distance lasers on a scaled railway vehicle[J]. Mechanical Systems and Signal Processing, 2020 138:106555.
15. Wu J, Zhu T, Wang Y, Lei C, Xiao S. TSVD Regularization-Parameter Selection Method Based on Wilson-θ and Its Application to Vertical Wheel-Rail Force Identification of Rail Vehicles[J]. Shock and Vibration 2022;Article ID 2598040:19 pages.
16. Mingmeng WA, Tao Z, Xiaorui WA, Shoune X. An inverse structural filter method for wheel-rail contact forces identification of railway vehicles[J]. J. Vib. Eng 2019;32:602-608.
17. Yabo Z. Research on wheel-Rail Force Inversion Method Based on Railway Vehicle Vibration Acceleration [D]. Southwest Jiaotong University, 2020.
18. Weixing C, Dong-run C, Zong-Shuai L. Aero engine Residual life prediction Method based on improved generative adversarial Network and ConvLSTM [J]. Journal of Electronic Measurement and Instrumentation 2023;37(03):211-221.
19. He Q, Sun H, Dobhal M, Li C, Mohammadi R. Railway tie deterioration interval estimation with Bayesian deep learning and data-driven maintenance strategy[J]. Construction and Building Materials 2022;342:128040.
20. Li Y, Liu J, Wang K, Lin J. Continuous measurement method of wheel/rail contact force based on neural network[M]//ICTE 2011:2533-2537.
21. Ranjia Z. Research on wheel-rail force measurement technology based on improved BP neural network [D]. Beijing Jiaotong University 2015.
22. Urda P, Aceituno J F, Muñoz S, Escalona JL. Artificial neural networks applied to the measurement of lateral wheel-rail contact force: A comparison with a harmonic cancellation method[J]. Mechanism and Machine Theory 2020;153:103968.
23. Teng F, Zhu R, Zhou Y, Chi M, Zhang H. A lightweight model of wheel-rail force inversion for railway vehicles[J]. Concurrency and Computation: Practice and Experience 2023;35(14):e6443.
24. Pires AC, Mendes GR, Santos GFM, Dias A. Indirect identification of wheel rail contact forces of an instrumented heavy haul railway vehicle using machine learning[J]. Mechanical Systems and Signal Processing 2021;160:107806.
25. Wu D, Ma X, Olson D L. Financial distress prediction using integrated Z-score and multilayer perceptron neural networks[J]. Decision Support Systems 2022;159:113814.
26. Ke L, Li M, Wang L, Deng S. Improved swarm-optimization-based filter-wrapper gene selection from microarray data for gene expression tumor classification[J]. Pattern Analysis and Applications 2023;26(2):455-472.
27. Maurya S and Verma NK. Intelligent Hybrid Scheme for Health Monitoring of Degrading Rotary Machines: An Adaptive Fuzzy c-Means Coupled With 1-D CNN," in IEEE Transactions on Instrumentation and Measurement 2023;72:1-10, Art no. 3510110.
28. Poostchi H, and Piccardi M. BiLSTM-SSVM: Training the BiLSTM with a Structured Hinge Loss for Named-Entity Recognition. IEEE Transactions on Big Data 2022;8(1):203-212.
29. Xu Q, Chen Z, Wu K, Wang C, Wu M and Li X. KDnet-RUL: A Knowledge Distillation Framework to Compress Deep Neural Networks for Machine Remaining Useful Life Prediction. IEEE Transactions on Industrial Electronics 2022;69(2):2022-2032.
30. Zheng W and Chen G. An Accurate GRU-Based Power Time-Series Prediction Approach With Selective State Updating and Stochastic Optimization. IEEE Transactions on Cybernetics 2022; 52(12):13902-13914.
31. Su Y, Shi W, Hu L and Zhuang S. Implementation of SVM-Based Low Power EEG Signal Classification Chip. IEEE Transactions on Circuits and Systems II: Express Briefs 2022;69(10):4048-4052.
32. Zhou Z, Zare R N. Personal information from latent fingerprints using desorption electrospray ionization mass spectrometry and machine learning[J]. Analytical chemistry 2017;89(2):1369-1372.
33. Zhang Y, Shi X, Zhang S, Abraham A. A xgboost-based lane change prediction on time series data using feature engineering for autopilot vehicles[J]. IEEE Transactions on Intelligent Transportation Systems 2022;23(10):19187-19200.

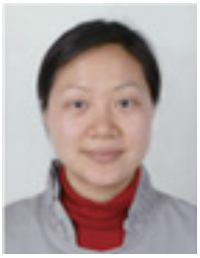

He Jing obtained M.Sc. Degree at Central South University of Forestry and Technology in 2002 and Ph.D. at National University of Defense Technology in 2009, respectively. Now she works as a professor at Hunan University of Technology. Her main research interests include electromechanical system fault diagnosis. E-mail: hejing@hut.edu.cn

Jia Lin (Corresponding Author): Obtained M.Sc. degree at Hunan University of Technology in 2014 and Ph.D. at Hunan University in 2021, respectively. Now he works as a lecturer at Hunan University of Technology. .His main research interests include parameter identification and control of heavy-haul trains
E-mail: jialin@ hut.edu.cn